Impact of Geomagnetically Induced Currents on Protection Current Transformers

B. Kasztenny, D. Taylor, and N. Fischer
Schweitzer Engineering Laboratories, Inc.

Presented at the
13th International Conference on Developments in Power System Protection
Edinburgh, United Kingdom
March 7–10, 2016

Impact of geomagnetically induced currents on protection current transformers

B. Kasztenny*, D. Taylor*, N. Fischer*

**Schweitzer Engineering Laboratories, Inc., 2350 NE Hopkins Court, Pullman, WA 99163 USA, doug_taylor@selinc.com*

Keywords: Geomagnetically induced current, current transformer, power system protection, dependability, security.

Abstract

This paper analyzes the performance of current transformers (CTs) under the presence of geomagnetically induced currents (GICs). Our intent is to characterize the impact of GICs on CT performance in the context of protection security and dependability. The paper proposes a simple CT model to analyze the GIC problem and applies it, as well as laboratory tests on a physical CT, to explain and quantify the impact of GICs on CTs. We conclude that GIC impact is negligible in steady states during load conditions or faults but is significant in the first few milliseconds of a fault. However, CT saturation caused by a preexisting GIC disappears very quickly. As a result, the impact to protective relays is minimal.

1 Introduction

Geomagnetically induced currents (GICs) are unipolar currents caused by earth's magnetic storms that flow in transmission lines and circulate through system grounding points, typically through wye-connected transformer windings and autotransformers. To the system, a GIC appears as a quasi-dc current superimposed onto the nominal system frequency currents. GICs remain a concern for the electric power industry, specifically with regard to the integrity of large, expensive, and difficult-to-replace assets (mainly power transformers and synchronous generators). In the case of power transformers, GICs can potentially cause thermal damage as a result of elevated excitation currents and stray flux closing outside of the transformer magnetic core. Further, the increased excitation current drawn by the transformers is harmonic-rich, which can cause problems for adjacent generators. In this case, the concern is the extra rotor heating caused by certain harmonic currents in the stator that establish a magnetic field rotating in the opposite direction of the rotor.

This paper focuses on the performance of current transformers (CTs) with GICs. In steady states, constant currents (such as GICs) are not transformed across the magnetic circuit of a CT, but they offset the magnetic flux and increase CT errors. Therefore, we are concerned with protection security and dependability for faults and switching events that happen when the primary current contains a GIC component.

The industry understands the impact of CT burden, CT ratio, saturation voltage, fault current level, system X/R ratio, or even remanent flux on the performance of protection CTs. We know how these factors contribute to CT saturation, and we can size a CT to avoid saturation or calculate the time to saturation for cases when saturation cannot be avoided [1].

However, the presence of GICs is a less understood factor that—at least in theory—impacts the performance of protection CTs. Our goal is to characterize that impact in both qualitative and quantitative manners so that we can combine our findings into a complete set of rating calculations for a CT (together with the burden, X/R ratio, saturation voltage, and so on).

In this paper, we briefly explain the GIC phenomenon and review the GIC levels we can expect in practice. Next, we introduce a novel and simplified CT model that allows us to understand and characterize the impact of GICs, as well as the impact of all traditional factors, such as the X/R ratio of the system, CT burden, or saturation voltage. We use this model in conjunction with tests on a physical CT to analyze the effects GICs have on a CT both in the steady state as well as transiently. We use these findings to provide CT derating rules that consider GICs and discuss the impact of GIC-induced CT errors on protective relays.

2 GIC phenomenon

Sunspots are regions of intense magnetic activity on the surface of the sun that result from spatiotemporal variations of the sun's magnetic field. Sunspots can produce a sudden release of energy in the form of solar flares and/or coronal mass ejections, which discharge large amounts of electrons, ions, and atoms. Once these particles reach the earth, they push on the earth's magnetosphere, and as a result, some of the particles enter the earth's ionosphere. This influx of charges changes the ionospheric current and the magnetic field it produces. As the time-varying magnetic field links conducting loops on the earth's surface (such as electrical transmission circuits, railways, or piping systems), the magnetic field induces an electromotive force around the loops, as dictated by Faraday's law. These geoelectric electromotive forces then drive GICs in the conducting circuits that superimpose onto the system currents.

GICs are especially noticeable in high-latitude locations (where the effects of geomagnetic storms are the greatest) and in long, high-voltage lines with tall transmission towers, both of which result in an increased loop area linked by the magnetic field, and therefore, an increased geoelectric electromotive force.

Because of the slow variation of the induced geoelectric field (relative to the power system frequency), a GIC is considered a quasi-dc current with frequencies in the millihertz range or lower. Fig. 1 is a capture of the GIC measured in a transformer neutral in Finland during a geomagnetic storm that occurred on March 24, 1991 [2]. The plot shows the erratic, yet very slowly changing, level of the induced current. For all practical purposes, GICs are preexisting dc currents when considering power system frequencies.

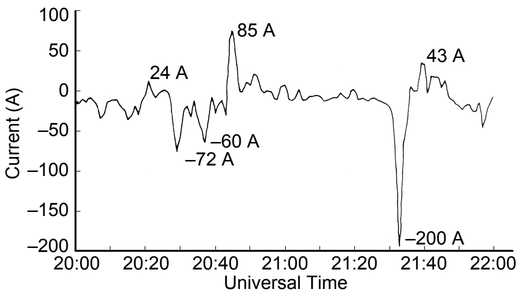

Fig. 1. GIC measured in a transformer neutral during a geomagnetic storm that occurred on March 24, 1991 [2].

When considering the magnitude of GICs, Fig. 1 provides an excellent example of severe GIC levels. In order to indicate their severity, geomagnetic storms are given a K-index rating. The storm that occurred on March 24, 1991, was a K-9 level storm, the highest level presently defined. The peak magnitude of –200 A that was captured in Fig. 1 represents a worst-case expected value. However, this value was measured in the transformer neutral, and the GIC present in each phase conductor is essentially one-third of this amount, or 67 A. This per-phase value corresponds to hand calculations of the GIC levels in the phase conductors given the magnetic field levels during a large geomagnetic storm and the resistance of a transmission line conductor [3].

Practically, when considering CTs, GICs are preexisting dc currents with magnitudes that are a small percentage (below 10 percent) of a typical transmission-grade CT rating.

3 Simplified CT model for protection considerations

A CT is a system with the primary current as an independent input, the secondary current as the output of interest, the burden, and the magnetic core all intertwined with the applicable laws of physics. The first approximation of this system, sufficient for protection studies, is as follows.

The primary (i_1) and secondary (i_2) currents follow the ampere-turn balance equation, with the excitation current (i_μ) modeling the core excitation and saturation. Typically, we have a single primary turn and *N* secondary turns, yielding the following:

$$i_1 = N \bullet (i_\mu + i_2) \quad (1)$$

Introducing the primary ratio current (i_1'), which is the ratio of i_1 to *N*, we can write (1) in secondary amperes as follows:

$$i_1' = i_\mu + i_2 \text{ or } i_2 = i_1' - i_\mu \quad (2)$$

Equation (2) signifies that the secondary current equals the primary ratio current less the excitation current. Therefore, the excitation current represents the CT error.

The secondary or excitation voltage (ν_2) of the CT is the product of the secondary current and the secondary burden (R_B), which is predominately resistive when considering microprocessor-based relays and which also includes the secondary winding resistance, the CT leads' resistance, and the relay input resistance. The secondary voltage of the CT is as follows:

$$\nu_2 = R_B \bullet i_2 \quad (3)$$

The induced excitation voltage is proportional to the rate-of-change of the magnetic flux; therefore, the magnetic flux linkage (λ) is an integral of the excitation voltage and is as follows:

$$\lambda = \int \nu_2 \, dt \quad (4)$$

Finally, we recognize the nonlinear relationship between the flux linkage and the excitation current as follows:

$$i_\mu = h(\lambda) \quad (5)$$

where *h* is the nonlinear function representing a relationship between the instantaneous excitation current and the instantaneous magnetic flux linkage (we neglect hysteresis because it is noncritical for our considerations).

Equations (1) through (5) are the first principles of a CT. We show them graphically in Fig. 2 using both the circuit model (a) and the signal model (b).

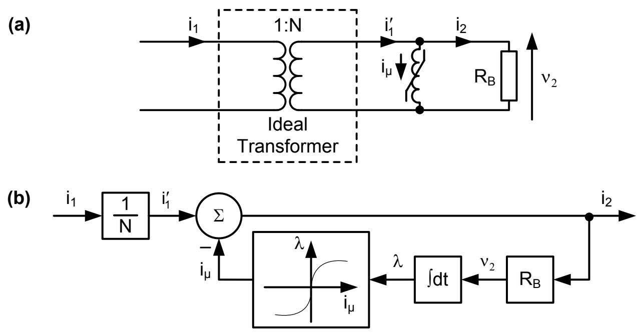

Fig. 2. CT representation using a circuit model (a) and a signal model (b).

The CT representation in Fig. 2b is helpful for understanding how CT errors are introduced in the first place. For small primary currents, the feedback in the form of the excitation current is small, making the secondary current practically equal to the primary ratio current. The higher the current, the higher the burden, and/or the lower the frequency, the larger the feedback and the resulting CT errors.

We tested the performance of our CT signal model by matching its *h* function to the 60 Hz excitation characteristic of a C10, 150:5 CT, as shown in Fig. 3. We selected a low-ratio CT in order to apply high multiples of rated current with our test equipment.

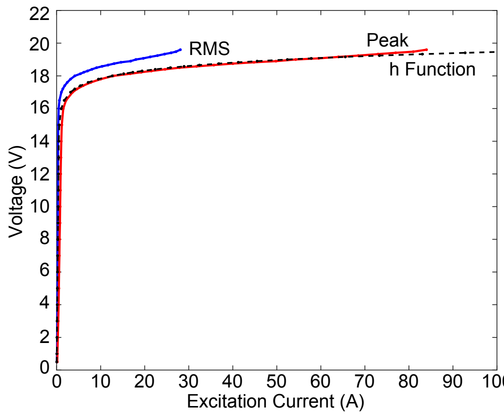

Fig. 3. Excitation characteristic (60 Hz) of the laboratory CT: measured excitation curves and best-fit *h* function (dashed line) for the CT model.

From Fig. 3, note the difference between the CT root-mean-square (rms) excitation curve, which is the curve used in standard practice, and its peak-valued excitation curve, which is the curve we must match the *h* function to in (5) for our CT model. The difference clearly illustrates the distortion of the excitation current once the CT operation passes its knee point and moves into the saturated region. Fig. 3 also shows that the *h* function for our CT model matches reasonably well to our laboratory CT (for comparison purposes, we scaled *h* from volt peak seconds [the unit for flux linkage] to volts rms).

To illustrate the accuracy of our simple model, we applied a fully offset fault current with a decaying dc component to both the laboratory CT and our CT model. The dc component had a 30 ms time constant and a magnitude of 1,350 A rms primary (9 times rated current and the maximum capacity of our laboratory equipment) at 60 Hz. Fig. 4a shows the individual CT responses to the fault. The plot shows that the CT model represents the laboratory CT reasonably well at 60 Hz. However, in order for our model to be useful in the analysis of CT performance when subjected to GICs, it needs to model the behavior for lower-frequency currents as well.

Fig. 4b captures the CT responses for a fault current of 30 Hz with a time constant of 60 ms and a current magnitude of 675 A rms primary (4.5 times rated current). As before, the model response reasonably matches that of the laboratory CT even at this lower frequency. How is this possible when the *h* function used in our model was matched with data at 60 Hz (see Fig. 3)?

The reason is that the *h* function is actually independent of frequency. The *h* function ties the flux linkage of the CT to its excitation current, as shown in (5). Because the CT flux linkage is the integral of the excitation voltage, as shown in (4), the frequency information that is present in the voltage signal is accounted for through the integration process. As the signal frequency decreases, the area under the excitation voltage waveform becomes larger (assuming that the voltage peak is held constant), resulting in a higher peak flux. The higher peak flux in turn requires a larger magnetizing current, as dictated by the frequency-independent *h* function.

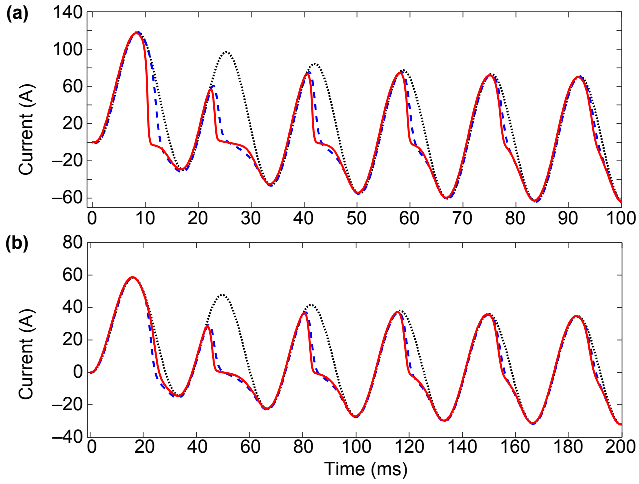

Fig. 4. Response of the laboratory CT and the CT model to 60 Hz fault current (a) and 30 Hz fault current (b): primary ratio current (black dotted), laboratory CT secondary current (red solid), and CT model secondary current (blue dashed).

This principle is the basis for the frequency derating of a CT. When reducing the signal frequency, we need to reduce the applied current proportionally (which reduces the excitation voltage proportionally) in order to keep the excitation current (i.e., the CT error), and thus the CT response, the same. This concept is depicted in Fig. 4, where the frequency and time constant were doubled and the current was halved in (b) in order to keep the CT response approximately the same as (a). More information and test results can be found in [4].

Having validated our CT model at nominal frequency, as well as at lower frequencies, we can now use it to study CT performance in the presence of GICs.

4 CT response to GICs

GICs change very slowly. We can approximate them with a dc component that is superimposed on the system nominal frequency current. In this section we analyze the steady-state and transient impact GIC has on CT operation.

4.1 CT steady-state response to GIC

Being a transformer, a CT does not reproduce a dc component in the steady state. However, when applying a dc step, a dc component flows initially in the secondary winding. This dc component creates a dc excitation voltage across the burden resistance. This voltage is integrated into a flux linkage, and therefore, the flux linkage ramps up linearly, drawing more and more excitation current. This continues until the CT reaches an equilibrium state in which the excitation current equals the primary ratio dc current, which forces the secondary dc current to zero (see Fig. 2b).

However, what happens if an ac signal is also present with the dc signal? This behavior is illustrated in Fig. 5, where we applied a primary current to our CT model, which was composed of 150 A dc superimposed with 150 A ac at 60 Hz (5 A dc and 5 A ac secondary).

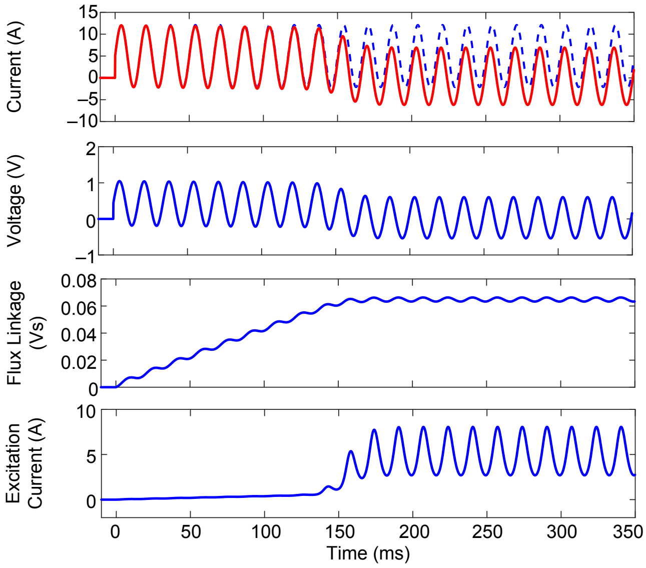

Fig. 5. Response of the CT model to a dc current of 150 A and an ac current of 150 A rms: primary ratio current (blue dashed), secondary current (red solid), secondary voltage, flux linkage, and excitation current.

In Fig. 5, note that initially the CT passes both the ac and dc components of the primary current. However, once the flux linkage builds up to approximately 0.06 Vs, it crosses the knee point of its excitation characteristic and there is a dramatic increase in the excitation current. Once this happens, the dc component disappears from the secondary current, but surprisingly, the magnitude reduction and angle shift in the 60 Hz secondary component are smaller than one might expect.

We filtered the primary ratio and secondary currents of Fig. 5 with a band-pass filter tuned to 60 Hz. We measured a magnitude error of 19 percent and a phase error of 31 degrees in the secondary current compared with the primary ratio current.

We explain the ability for the CT to simultaneously be saturated in terms of the dc component while still reproducing the 60 Hz component reasonably well by pointing out the difference in flux linkage that each component produces. Supporting the 150 A dc component in the primary signal results in a flux linkage of 0.065 Vs, as indicated by the dc component of the flux linkage in Fig. 5 once steady state is reached. However, the 150 A ac component only results in a peak flux linkage of 0.00162 Vs (consider the area under the ac portion of the excitation voltage of Fig. 5 compared with the area under the dc portion). This ac flux linkage superimposes around the dc bias of 0.065 Vs, as shown in Fig. 5. While the CT is operating in the saturated region at this point, it is able to support the small oscillation of the ac component with surprising accuracy. This behavior was also observed in [5].

4.2 Derating a CT for steady-state GIC effects

To magnify the effect GICs have on steady-state CT performance, the previous example assumed an unrealistic GIC current whose magnitude was equal to the rated current of the CT. In practice, a GIC component is 10 percent or less of the CT rated current. For example, a 50 A dc per-phase current in a transmission line protected using 800:5 CTs is only 50 / 800 = 6.25 percent of the rated current. This low bias impacts CT performance under fault conditions to a very small degree, as we will now illustrate.

The "no-saturation" CT operating condition is specified by the CT error being below 10 percent. We use the 10 percent difference between the primary ratio current magnitude and the secondary current magnitude as the limit of no-saturation operation. To obtain our reference value (no GICs present), we increase the CT burden to the point that we obtain 10 percent error at exactly 20 times rated current. Then we step through a range of GIC values for our CT model and find—for each GIC value—the symmetrical ac current that brings us to the 10 percent error. Table 1 shows the results.

I_{GIC} (pu)	I_{AC} (pu)
0	20.00
0.1	20.00
0.2	19.99
0.3	19.99
0.4	19.98
0.5	19.98
0.6	19.94
0.7	19.73
0.8	19.25
0.9	18.59

Table 1: Maximum ac reproduced with 10 percent error for a given GIC (C10, 150:5 CT).

The results show that for realistic values of the GIC (0 to 10 percent of rated current), the impact is unnoticeable. However, if the amount of GIC approaches the CT nominal current, the impact is certainly observable, as Fig. 5 demonstrated.

4.3 CT transient response to GICs

Having examined the steady-state effects GICs have on CTs, we now turn our attention to the transient effects. To demonstrate these effects, we applied a prefault load current of 150 A rms (rated current) to the laboratory CT and then applied a symmetrical fault current of 1.6 kA. We recorded the CT response for two different cases: (1) no GICs present in the primary current, and (2) a GIC of 15 A dc (10 percent of rated current). Fig. 6 captures the two responses.

Congruent with the previous subsection, Fig. 6 shows that in the steady state, the ac component with a GIC present is reproduced well compared with the ac component without

GIC present (note the slightly elevated steady-state excitation current levels in the GIC case). However, the transient response during the first half-cycle of the fault is quite different; the transient saturation of the CT is much more severe when the GIC is present.

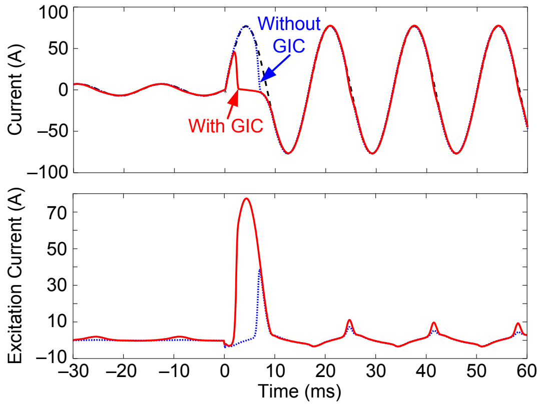

Fig. 6. Laboratory CT response with and without a GIC of 15 A dc present during a prefault load of 150 A rms and fault current of 1.6 kA rms: primary ratio current (black dashed), secondary current without GIC (blue dotted), secondary current with GIC (red solid), excitation current without GIC (blue dotted) and excitation current with GIC (red solid).

The reason for this dramatic difference is that, while the GIC magnitude is small in comparison with the CT capacity (10 percent of rated current), the GIC creates a significant bias in the flux linkage level of the CT prior to the fault. For our laboratory CT, the 15 A dc offsets the flux linkage by a value of 0.053 Vs. In comparison, the knee-point flux linkage level is around 0.06 Vs. Then, because the first half-cycle polarity of the fault current is the same as that of the GIC, the flux linkage level quickly moves past the knee point, resulting in the severe transient saturation observed. This effect is very similar to the transient saturation experienced by a CT with a large remanent flux left in its core when it is exposed to fault current, as demonstrated in Fig. 7.

The upper plot of Fig. 7 shows the performance of our CT model under an ac current of 10 times rated with remanent flux linkages of 0.00, 0.01, 0.02, 0.03, 0.04, and 0.05 Vs. The higher the remanent flux, the more significant the transient saturation. What is important to notice is that the CT recovers from the transient saturation within about a half-cycle, just as we observed when a GIC was present in Fig. 6.

Fig. 7 gives us insight into why the transient saturation experienced by the CT when exposed to a GIC or remanent flux is short-lived. Let us focus on the CT secondary current for the case where the remanent flux linkage is 0.05 Vs. The flux linkage for this case is given in the bottom plot of Fig. 7. When the current is applied, the flux linkage increases from its initial value of 0.05 Vs to about 0.065 Vs (an amount proportional to the positive portion of the secondary current marked as Area 1). However, at this flux linkage level, the CT draws a very large excitation current, which causes the sharp drop in the secondary current. Once the secondary current becomes negative, the flux linkage decreases by a value proportional to the negative portion of the current (Area 2). Because Area 2 is considerably larger than Area 1, the flux linkage decreases to well below the initial value of 0.05 Vs. This situation repeats as long as the CT goes into saturation. As a result, the CT has an inherent tendency to remove the transient saturation caused by remanent flux and/or GICs.

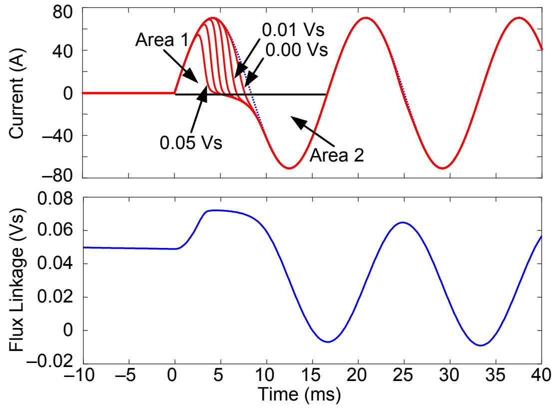

Fig. 7. Response of the CT model to a fault current of 10 pu rms with a remanent flux linkage between 0.00 Vs and 0.05 Vs: primary ratio current (blue dotted), secondary current (red), and flux linkage for the 0.05 Vs remanent flux case.

4.4 Derating a CT for transient GIC-induced saturation

As previously described, a GIC offsets the flux linkage of a CT by an amount dictated by the excitation characteristic of the core. This offset decreases the room available to accommodate the fault current without saturation. We offer the following procedure to evaluate the derating factor for the transient CT performance caused by a GIC.

From the excitation curve plotted using peak excitation current values (the red curve in Fig. 3), we can read the rms voltage corresponding to the GIC level in question. For example, for the 10 percent GIC level in our laboratory CT (0.5 A), we see from Fig. 3 that a voltage of 14 V rms is required. This is the voltage level that is effectively used up in the CT because of the GIC. When considering transient saturation, this voltage translates into a current level the CT is no longer able to support, as determined by the burden resistance. Given the burden we used with our CT model to achieve a 10 percent error at 20 times rated current, the 14 V level in our example corresponds to a current of 73 A rms secondary, or 14.6 pu. Thus, the 0.1 pu GIC is equivalent to an ac current of 14.6 pu rms.

This example shows that the impact of GICs is significant. To remove the transient effect of a GIC component of only 10 percent of CT rated value, we need to reduce the ac component by 14.6 times the CT rated value.

5 Impact of GIC-induced CT errors on protection

In the previous sections, we explained that steady-state CT errors caused by practical GIC levels are minor. Protective relays are not designed or applied assuming perfect CT performance. Both design and setting margins are applied to cope with CT ratio errors and CT saturation.

We conclude the following with respect to protection elements that can be impacted by steady-state CT saturation caused by GICs:

- Line distance and overcurrent elements may slightly underreach due to CT errors caused by GICs. However, these elements do underreach under normal conditions (such as fault resistance) and are therefore backed up by other protection elements. Time-coordinated elements apply margins, and they retain dependability despite the GIC-caused CT errors.
- Line differential elements typically incorporate a means to address CT saturation, such as percentage restraint or the Alpha Plane [6], and they comfortably tolerate CT errors caused by GICs in steady states.
- Transformer differential elements include percentage restraint to cope with CT errors, and they too remain secure for external faults, even under GICs.

Transient CT saturation due to preexisting GICs can be substantial. The saturation is, however, short-lived. We offer the following comments with respect to this:

- Distance and overcurrent relays tend to underreach because of substantial CT saturation in the first half-cycle of the fault current. As a result, we may see slightly delayed protection operation for in-zone faults due to transient CT saturation caused by GICs. Again, the instantaneous distance and overcurrent elements can underreach (e.g., during resistive faults), and their slightly delayed operation will therefore not cause major problems and is not typically even noticed.
- Fast line differential relays may be affected by transient CT saturation, but these relays already guard against CT saturation when designed properly. Slower line differential relays are secure because the errors during transient CT saturation from GICs are short-lived.
- Similar points apply to transformer differential relays.

We conclude that the impact of GIC-induced CT saturation on protective relays is minor. Existing means to deal with CT saturation caused by more common factors ensure security for CT errors caused by GICs.

6 Conclusion

This paper provides a methodology to analyze the impact of GICs on protection CTs and makes a number of observations related to the topic.

The presented signal model of a CT is a very useful way of depicting the operation of a CT and aids understanding of CT operation for a number of conditions and factors.

Practical GIC levels have a minor impact on transmission-rated CTs in steady states. Transiently, even small GIC levels can lead to CT saturation during faults, but the CT pulls out of this GIC-induced saturation very quickly (in a half-cycle). While this effect is significant, it is similar to the impact of remanent flux, and it does not bring any new threats to properly designed protection systems.

The paper also provides a methodology to derate a CT for the expected level of a GIC. When applied to guarantee saturation-free CT operation, this methodology leads to a considerably oversized CT (similar to factoring in a high remanent flux). We do not recommend applying such derating. Without the derating, the CT may experience saturation, but the saturation quickly disappears.

Ultimately, our takeaways agree with common observations and the lack of correlation between days of high geomagnetic activity and relay misoperations. We analyzed our data on unexpected relay operations and magnetic storm activity but found no correlation.

References

[1] H. J. Altuve, N. Fischer, G. Benmouyal, and D. Finney, "Sizing Current Transformers for Line Protection Applications," proceedings of the 66th Annual Conference for Protective Relay Engineers, College Station, TX, April 2013.

[2] J. Elovaara, P. Lindblad, A. Viljanen, T. Mäkinen, R. Pirjola, S. Larsson, and B. Kielén, "Geomagnetically Induced Currents in the Nordic Power System and Their Effects on Equipment, Control, Protection and Operation," proceedings of the CIGRE 1992 Session, Paper 36-301, Paris, France, August 1992.

[3] R. Pirjola, "Geomagnetically Induced Currents During Magnetic Storms," I*EEE Transactions on Plasma Science*, Vol. 28, Issue 6, December 2000, pp. 1867–1873.

[4] B. Kasztenny, N. Fischer, D. Taylor, T. Prakash, and J. Jalli, "Do CTs Like DC? Performance of Current Transformers With Geomagnetically Induced Currents," proceedings of the 42nd Annual Western Protective Relay Conference, Spokane, WA, October 2015.

[5] J. G. Kappenman, V. D. Albertson, and N. Mohan, "Current Transformer and Relay Performance in the Presence of Geomagnetically-Induced Currents," *IEEE Transactions on Power Apparatus and Systems*, Vol. PAS-100, Issue 3, March 1981, pp. 1078–1088.

[6] B. Kasztenny, G. Benmouyal, H. J. Altuve, and N. Fischer, "Tutorial on Operating Characteristics of Microprocessor-Based Multiterminal Line Current Differential Relays," proceedings of the 66th Annual Georgia Tech Protective Relaying Conference, Atlanta, GA, April 2012.

20151117 • TP6740